International Journal of Nanomedicine

Dovepress

open access to scientific and medical research

Open Access Full Text Article

ORIGINAL RESEARCH

Characterization of Nanohybridosomes from Lipids and Spruce Homogenate Containing Extracellular Vesicles

Vesna Spasovski[1,2,*], Anna Romolo[1,3,*], Urška Zagorc[4], Vesna Arrigler[4], Matic Kisovec[5], Apolonija Bedina Zavec[5], Matevž Arko[1], Adrienn Molnár[6,7], Gitta Schlosser[7], Aleš Iglič[3,8], Ksenija Kogej[4], Veronika Kralj-Iglič[1]

[1]University of Ljubljana, Faculty of Health Sciences, Laboratory of Clinical Biophysics, Ljubljana, Slovenia; [2]Institute of Molecular Genetics and Genetic Engineering, University of Belgrade, Belgrade, Serbia; [3]University of Ljubljana, Faculty of Electrical Engineering, Laboratory of Physics, Ljubljana, Slovenia; [4]University of Ljubljana, Faculty of Chemistry and Chemical Technology, Ljubljana, Slovenia; [5]National Institute of Chemistry, Department of Molecular Biology and Nanobiotechnology, Ljubljana, Slovenia; [6]Hevesy György PhD School of Chemistry, ELTE Eötvös Loránd University, Budapest, Hungary; [7]MTA-ELTE Lendület Ion Mobility Mass Spectrometry Research Group, Faculty of Science, Institute of Chemistry, ELTE Eötvös Loránd University, Budapest, Hungary; [8]University of Ljubljana, Faculty of Medicine, Laboratory of Clinical Biophysics, Ljubljana, Slovenia

*These authors contributed equally to this work

Correspondence: Veronika Kralj-Iglič, Email veronika.kralj-iglic@zf.uni-lj.si

Introduction: Lipid nanovesicles associated with bioactive phytochemicals from spruce needle homogenate (here called nano-sized hybridosomes or nanohybridosomes, NSHs) were considered.

Methods: We formed NSHs by mixing appropriate amounts of lecithin, glycerol and supernatant of isolation of extracellular vesicles from spruce needle homogenate. We visualized NSHs by light microscopy and cryogenic transmission electron microscopy and assessed them by flow cytometry, dynamic light scattering, ultraviolet–visual spectroscopy, interferometric light microscopy and liquid chromatography–mass spectrometry.

Results: We found that the particles consisted of a bilayer membrane and a fluid-like interior. Flow cytometry and interferometric light microscopy measurements showed that the majority of the particles were nano-sized. Dynamic light scattering and interferometric light microscopy measurements agreed well on the average hydrodynamic radius of the particles R_h (between 140 and 180 nm), while the concentrations of the particles were in the range between 10^{13} and 10^{14}/mL indicating that NSHs present a considerable (more than 25%) of the sample which is much more than the yield of natural extracellular vesicles (EVs) from spruce needle homogenate (estimated less than 1%). Spruce specific lipids and proteins were found in hybridosomes.

Discussion: Simple and low-cost preparation method, non-demanding saving process and efficient formation procedure suggest that large-scale production of NSHs from lipids and spruce needle homogenate is feasible.

Plain Language Summary: Cells shed into their exterior nanoparticles (here referred to as extracellular vesicles – EVs) that are free to move, reach distant cells and are taken up by them. As they carry bioactive constituents, EVs may have important impact on the recipient cells. The mechanisms of EV formation and mediation can be employed in designing therapeutic, prophylactic and diagnostic methods for various medical issues. EVs can be harvested from biological samples; however, their yield is small,[12] and there are potential side effects. Artificial vesicles – liposomes – have high yield; however, in vivo, they can be degraded before reaching the target and their reproducibility is yet insufficient. In order to combine advantages of both types of nanoparticles, we have composed nanohybridosomes (NSHs) from soya lecithin, water and supernatant of isolation of EVs from spruce needle homogenate, visualized them by cryogenic electron microscopy and characterized them with respect to their size, concentration and protein/nucleic acid content. We have applied a recently developed interferometric light microscopy to determine the hydrodynamic radius and the concentration of EVs. We found that the majority of composed particles are nano-sized and that they enclose more than 25% of the incoming volume of liquid, which is

Received: 28 July 2023
Accepted: 15 December 2023
Published: 22 February 2024

considerably more than about 1% that can be harvested by isolation of EVs from spruce needle homogenate by (ultra) centrifugation.

Keywords: hybridosomes, liposomes, nanovesicles, extracellular particles, small cellular particles, drug delivery

Introduction

In cell-to-cell communication, cells constantly exchange matter and information by means of their fragments (extracellular vesicles, EVs) which after detachment from the mother cell become free to move and interact with other cells. The mechanisms of cell fragmentation, fission of EVs from the mother cell and interaction of EVs with recipient cell may be non-specific as regards the molecular composition of EVs and therefore form an ancient evolutionary conserved language that all involved organisms can understand. Acknowledging and learning the natural laws that underlie this mechanism are prerequisite for the development of effective therapeutic, prophylactic and diagnostic methods in human, animal and plant nanomedicine.[3–6] Therefore, EVs have recently been considered as potential key players in addressing different diseases.[7–12] Advantages of EVs are their ability to deliver to the cells biologically active substances that would without shielding be degraded by enzymes, unable to traverse the cell membrane or induce immune responses. Disadvantages of EVs are their considerable complexity and potential high chance of side effects.[1] Moreover, a noticeable obstacle in this promising area is the fact that the yield of vesicles isolated from natural sources is usually very small.[2] While chemical and mechanical treatment were shown to increase the concentration of EVs in isolates[13] and different methods and protocols have been elaborated to harvest EVs from natural sources, in some systems considered, they have up to now failed to reach large-scale level.[14]

In contrast, liposomes are already being used in clinical practice, mainly due to their high yield, but also for their stability, simplicity of preparation, high drug-loading efficiency, bioavailability and safe use.[15] Lecithins from soya or eggs have previously been investigated for topical use and showed good tolerance and no toxicity to cells.[16,17] Such liposomes were reported to deliver active ingredients across cell membranes, and their effects differed with respect to different formulations.[16,17] In loading into liposomes, hydrophobic cargoes were found to be readily dissolved within the phospholipid mixture and hydrophilic cargoes were inserted in the aqueous media and then integrated into the liposomes while being hydrated.[18,19] It is considered that the lipid bilayer of the liposome membrane can protect the encapsulated cargo from degradation by enzymes.[20] It was found that in the intestine, liposomes can bind to mucosa[21] and transport bioactive substances into the cells.[22] Different natural and artificial nanoparticles are being considered for carriers of anti-cancer drugs[23,24] and have already been used in delivery of mRNA in the development of COVID-19 vaccine.[25] Shortcomings of liposomes are accelerated blood clearance and insufficient reproducibility.

Optimal carriers would integrate advantages of EVs and liposomes to form functional EV mimetics of low complexity and well-characterized components. There is urgent need to better understand the mechanisms of carrier formation as to improve large-scale technologies for production of delivering particles[26] and enrichment of their inner compartment with biogenic molecules.[27] By appropriate engineering and/or selection of the cells that are the source of EVs, various forms of particles have been considered[27] eg synthetic vesicles, natural extracellular particles and their combinations.[28] Synthetic vesicles mimic natural ones in terms of biological activity but could be synthesized in higher amounts and filled intentionally with specific and desirable cargo[29,30] Combination of vesicles of natural origin and synthetic ones would circumvent robust cellular manipulation needed for isolation of natural extracellular particles[29,31] (which is usually expensive and time-consuming) and enable synthetic nanocarriers to entrap biologically active molecules.[5,29] Employment of this nanotechnological strategy could generate efficient and reproducible biocompatible carriers for downstream applications, which are here referred to as nanohybridosomes.

Plants use extracellular vesicles to pack and secrete their active compounds such as DNA, RNA, miRNA, lipids, proteins, and metabolites[32,33] that exhibit anti- inflammatory, anti-fungal and anti- insecticide effect but also can have cancer-protective and many other properties important for health and environment.[34–37] In this respect, European spruce (*Picea abies*) is a rich source of compounds that can be pharmacologically active. Essential oils of *Picea abies* constitute mostly of monoterpenes,[38] among which limonene is shown to drive antimicrobial activity.[39] Therapeutic potential of

pinenes, the most representative monoterpenes in *Picea abies* essential oils, was shown to exhibit anti-fungal and antimicrobial activity.[40] α- and β- Pinene were reported anti-inflammatory, antibacterial, antioxidant, anticancer, and also antibiotic resistance modulator activity.[41–45]

Recently, EVs were isolated from homogenate of *Picea abies* needles by differential ultracentrifugation.[46] During the procedure, cellular debris and larger particles are removed but the sample may contain fraction of the smallest explosive EVs (resulting after cell mechanical disruption). Electron micrographs revealed the presence of different types of nanoparticles in the samples.[46–48] The isolate and the supernatant of the last step of ultracentrifugation contained electron dense particles and bilayer membrane-enclosed nanovesicles, but the yield (volume and concentration) of these naturally composed particles was low.[46] However, the supernatants of the isolation procedure contained terpenes and flavonoids.[46] The purpose of this work was to develop an efficient but simple and low-cost method for the formation of NSHs that could deliver the beneficial cargo to cells. The idea is to enclose the natural compounds into NSHs in which membranes would be composed mainly of artificially added lipids. EVs may merge with or be included in NSHs but as their proportion with respect to liposomes would be small, they are not expected to be the main determinant of the morphology, yield and membrane composition of the NSHs. In contrast, the aqueous portion of NSHs, enclosed within the lipid bilayer-based membrane, comes from the natural source as there are no other aqueous solution ingredients included in the preparation. NSHs derived in this way should have characteristics of both natural and synthetic vesicles. For comparison, we have prepared and characterized also liposomes from lecithin, water and glycerol.

Materials and Methods

Scheme for preparation of nanohybridosomes is depicted in Figure 1.

Chemicals

Edible soya lecithin was from Fiorentini, Torino, Italy. Egg lecithin was from Sigma Aldrich, St. Louis, USA 61,755–25G, USA, with an L-α-phosphatidyl choline content 82.9%. Protein standard was from Sigma Aldrich, St. Louis, USA P5369-10ML.

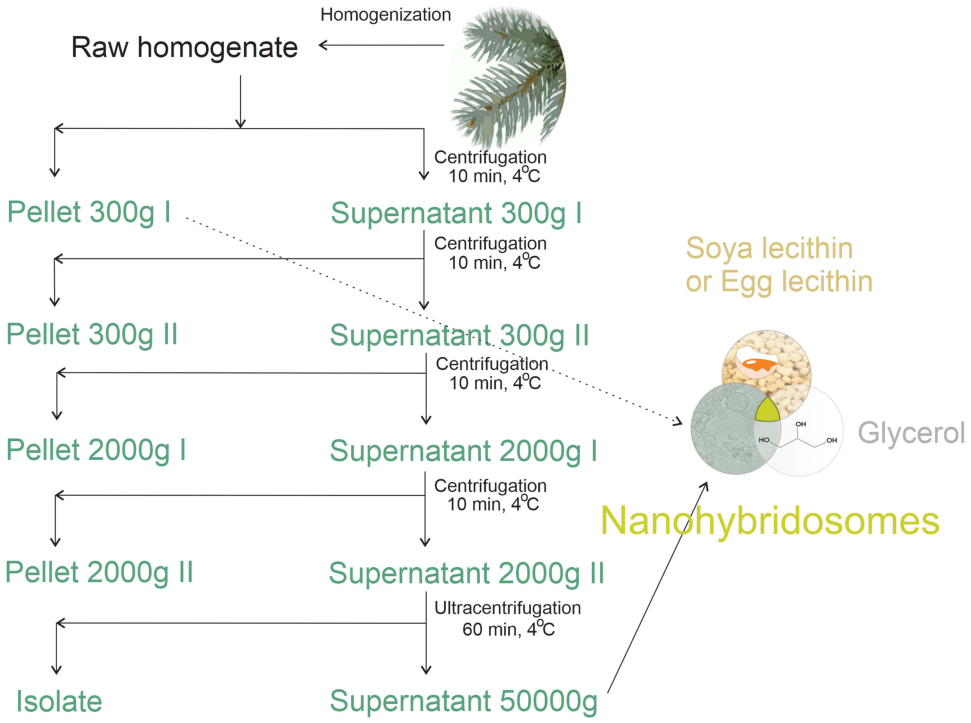

Figure 1 Scheme of the procedure for assembling nanohybridosomes from lecithin, glycerol and supernatant or pellet from spruce needle homogenate.

Preparation of Spruce Needle Homogenate

About 50 g of dry weight of *Picea abies* tree branches were immersed into water with dissolved sodium hypochlorite (NaClO, 0.1%) at about 30 °C for about 1 hour. The branches were washed with water. The needles were removed from the branches by cutting. The cut needles were added to 300 mL of ultra-clean water (B. Braun, Melsungen, Germany) and stirred with the KOIOS 850W Smoothie Bullet Blender (KOIOS, Newegg, USA) for 30 seconds. The homogenate was filtered by free flow of the fluid through 0.5 mm nylon net cloth in order to remove larger particles.

Isolation of Small Cellular Particles from Spruce Needle Homogenate

Small cellular particles were obtained by isolation using differential centrifugation. An adapted protocol for isolation of extracellular vesicles (Figure 1) [49] was followed. The homogenate was centrifuged at 300 g and 4°C for 10 minutes in the centrifuge Centric 260R with rotor RA 6/50 (Domel, Slovenia). Fifty-milliliter conical centrifuge tubes (ref. S.078.02.008.051, Isolab Labor-geräte GmbH, Germany) were used. The procedure was repeated twice. The supernatant of the second centrifugation at 300 g was centrifuged at 4°C and 2000 g for 10 minutes in the centrifuge Centric 400R with rotor RS4/100 (Domel, Slovenia). Fifteen-milliliter conical centrifuge tubes (ref. S.078.02.001.050, Isolab Laborgeräte GmbH, Germany) were used. The procedure was repeated twice. The supernatant was centrifuged at 4°C and 50,000 g for 60 min in Beckman L8-70M ultracentrifuge, rotor SW55Ti (Beckman Coulter, USA). Thin-wall polypropylene centrifuge tubes (ref. 326819, Beckman Coulter, USA) were used. The supernatant (or 300g I pellet in the case of dilution experiment for flow cytometry) was used in the formation of NSHs (Figure 1).

Preparation of NSHs and Liposomes

We prepared liposomes by mixing appropriate proportions of lyophilized granules of soya lecithin with ultra-clean water (B Braun, Melsungen, Germany)/supernatant from spruce needle homogenate, and glycerol (Figure 1) at equal weight proportions (2 g).[50] The substances were mixed at room temperature. Water/supernatant was poured onto lecithin and left standing at room temperature for 1 hour. Then, we added glycerol and mixed the sample by pipetting with Pasteur pipette (in the case of NSHs) or metallic spoon (in the case of liposomes). To prevent blocking of the tubes of the flow cytometer and strong absorption of light for the needs of UV-vis and interferometric light microscopy, and to homogenize the samples, the samples were filtered through 0.8, 0.45 and 0.2 μm filters manually by using a syringe. We have imaged also liposomes that were stored in a falcon tube as prepared (undiluted) at room temperature for 6 months.

Light Microscopy

The samples were observed under Nikon EM CCD inverted optical microscope (Eclipse TE2000-S, Tokyo, Japan; equipped with a digital spot boost Visitron Systems camera system).

Cryogenic Transmission Electron Microscopy

C-flat™ 2/2, 200 mesh holey carbon grids (Protochips, Morrisville, NC, USA) were glow-discharged for 60 s at 20 mA, air atmosphere, positive polarity (GloQube ® Plus, Quorum, Laughton, UK). We applied 3 μL of sample to the grid. Then, the sample was blotted and vitrified in liquid ethane on Vitrobot Mark IV (Thermo Fisher Scientific, Waltham, MA, USA). Vitrobot conditions were as follows: 100% relative humidity, blot force: 2, blot time: 7 s and 4 °C. Samples were visualized under cryogenic conditions. We used a 200 kV Glacios microscope with Falcon 3EC detector (Thermo Fisher Scientific, Waltham, MA, USA).

Flow Cytometry

Flow cytometry was performed according to the protocol adapted from Škufca et al[51] by MACS QUANT (Miltenyi, Bergisch-Gladbach, Germany) flow cytometer. For calibration, we used beads of sizes 2 and 3 μm (MACSQuant Calibration Beads, ref: 130–093-607). The setting of the lasers was 458 V (FSC) and 467 V (SSC). The setting of the SSC trigger was 1.800. The estimation of the dilution range appropriate to measure the samples is given in Supplementary material, Figure S1 and the scatter diagrams for two example samples are given in Figure S2.

Ultraviolet Spectroscopy (UV-VIS)

Two microliters of the sample was applied to a NanoDrop UV spectrometer (Thermo Fisher Scientific, Waltham, Massachusetts, USA) which detects ultraviolet-visible spectrum (UV-Vis) absorbance. The equipment was set for assessment of protein content as explained in https://tools.thermofisher.com/content/sfs/brochures/Thermo-Scientific-NanoDrop-Products-Protein-Technical-Guide-EN.pdf.

Dynamic Light Scattering

Diluted NSH and liposome samples were examined by Dynamic Light Scattering[52,53] using Instrument 3D-DLS-SLS cross-correlation spectrometer (LS Instruments GmbH, Fribourg, Switzerland) with a 100 mW, $\lambda_0 = 660$ nm DPSS laser (Cobolt Flamenco, Cobolt AB, Sweden). Light scatters stronger by larger particles and if present in the samples, the signal from larger particles prevents measurement of smaller ones.[54,55] Therefore, before measurements, samples were gently filtered through 450 nm low protein-binding Millex filters directly into the measuring cuvette. The samples were equilibrated in a decalin bath at 25 °C for 15 min. The scattered light was measured for 120 s at an angle $\theta = 90°$. The analysis was performed by a software based on the inverse Laplace transform program CONTIN Polymer 2014 created in-house. For each setting, we collected several intensity correlation functions (CFs) which were fitted with up to 50 exponents. Individual CFs were subjected to independent analysis and compared with the averaged curve. We obtained the values of the hydrodynamic radius of EVs (R_h) from the diffusion coefficients (D) assessed from the calculated correlation function ($g_1(t)$), obtained from the measurement of the scattered light intensity $g_2(t)$. We used the Siegert's relation and the Stokes-Einstein equation ($R_h = kT/6\pi\eta D$, where k is the Boltzmann constant, T is the absolute temperature, and η is the viscosity of the medium). The viscosity of the medium was taken to be equal to the viscosity of water at 25°C.

Interferometric Light Microscopy

The average hydrodynamic radius (R_h) and the concentration of liposomes were assessed by interferometric light microscope (Videodrop, Myriade, Paris, France). Signal of the medium (ultra-clean water) was under the detection limit. We set the threshold value to 4.2. We applied 5–10 µL of the sample between cover glasses and illuminated it by 2W blue LED light. The scattered light interfering with the incoming light was detected by a complementary metal–oxide–semiconductor high resolution high speed camera. The image was processed by computer to identify the particles and their positions. The number of the particles in a given volume (typically 15 pL) was taken as the concentration of the particles. Video films were taken to track the particles. The trajectories of the particles were analyzed by assuming that the particles are undergoing Brownian motion reflecting the temperature of the sample. The diffusion coefficient D of the motion of the particle was taken to be proportional to the mean square displacement d of the particle in the time interval between two consecutive frames Δt, $\langle d^2(\Delta t)\rangle = \langle 4D\,\Delta t\rangle$. The particles were assumed to be spherical. The Stokes–Einstein relation ($R_h = kT/6\pi\eta D$) was used. The particles were tracked and processed individually. The software QVIR 2.6.0 (Myriade, Paris, France) was used to perform the analysis.

Liquid Chromatography-Mass Spectrometry (LC-MS) Lipid Profiling

100–100 µL of the spruce needle homogenate sample, 100–100 µL of the 50,000g supernatant of the EV isolation procedure and 100–100 mg of the hybridosome samples were examined. First, 150 µL methanol was added to the samples, vortexed, then 500 µL tert-Butyl methyl ether (MTBE) was added and the samples were incubated in a mixer (Eppendorf Thermomixer, Eppendorf, Hamburg, Germany) at 600 rotations per minute (rpm) for one hour at room temperature. 125 µL water was added to the samples and after 10 minutes of incubation at room temperature, samples were centrifuged in an Eppendorf 5430R centrifuge (Eppendorf, Hamburg, Germany) at 13,000 g for 10 minutes. The upper organic phase containing the lipid fraction was collected, and samples were dried in a vacuum centrifuge (Eppendorf 5430R, Eppendorf, Hamburg, Germany). Samples were dissolved in 150 µL of the starting eluent mixture used in the High-Performance Liquid Chromatography (HPLC) separation.

HPLC-MS measurements were performed on a high resolution and high mass accuracy Q-Exactive Focus hybrid quadrupole-orbitrap mass spectrometer (Thermo Fisher Scientific, Bremen, Germany) equipped with heated electrospray ionization source. The mass spectrometer was coupled to a Dionex 3000+ UHPLC system. For the separation, a Waters ACQUITY UPLC CSH C_{18}, 2.1×100 mm, 1.7 µm column was used, and the column temperature was 55 °C. Gradient elution was used with a flow rate of 400 µL/min. Mobile phase A was 600/390/10 (Acetonitrile/Water/1 M aqueous ammonium formate) containing 0.1% formic acid

(V/V), mobile phase B was 900/90/10 (Isopropanol/Acetonitrile/1 M aqueous ammonium formate) containing 0.1% formic acid (V/V). The gradient program was the following: 50% B eluent at 0 min, 53% at 0.5 min, 55% at 4 min, 65% at 7 min, 80% at 7.5 min, 99% at 10 min, 99% at 11 min, 50% at 12 min, 50% at 15 min. Waters Progenesis QI program was used for data analysis.

Results

Light microscopy and cryogenic transmission electron microscopy images of NSHs prepared from soya lecithin, glycerol and supernatant of 50,000 g isolation from spruce needle homogenate are shown in Figure 2. The mixture appeared as a brownish cream. When directly applied to the cover glass and observed by light microscopy, the texture was largely uniform (Panel A). Rounded texture is visible at higher magnification (Panels B and C). Dilution with water resulted in separated regions of material (Panel D). For observation with cryogenic transmission electron microscopy, the samples were diluted 50,000×. Panels E-G show low magnification images of the fresh samples. Higher magnification reveals the presence of nanovesicles enclosed by a bilayered membrane (Panels H, I, K) and a few small electron dense particles (Panel K, black arrow). Many vesicles are adhered to each other (Figure 2H and I). This feature was previously observed in giant unilamellar vesicles observed under light microscopy (Panel J). In giant unilamellar vesicles, the form of double bubble (Panel J) was outlined[56] while in NSHs that we observed in this study the interface between the vesicles was often bent towards the larger vesicle (Panel K). Some smaller vesicles appeared as if they were being

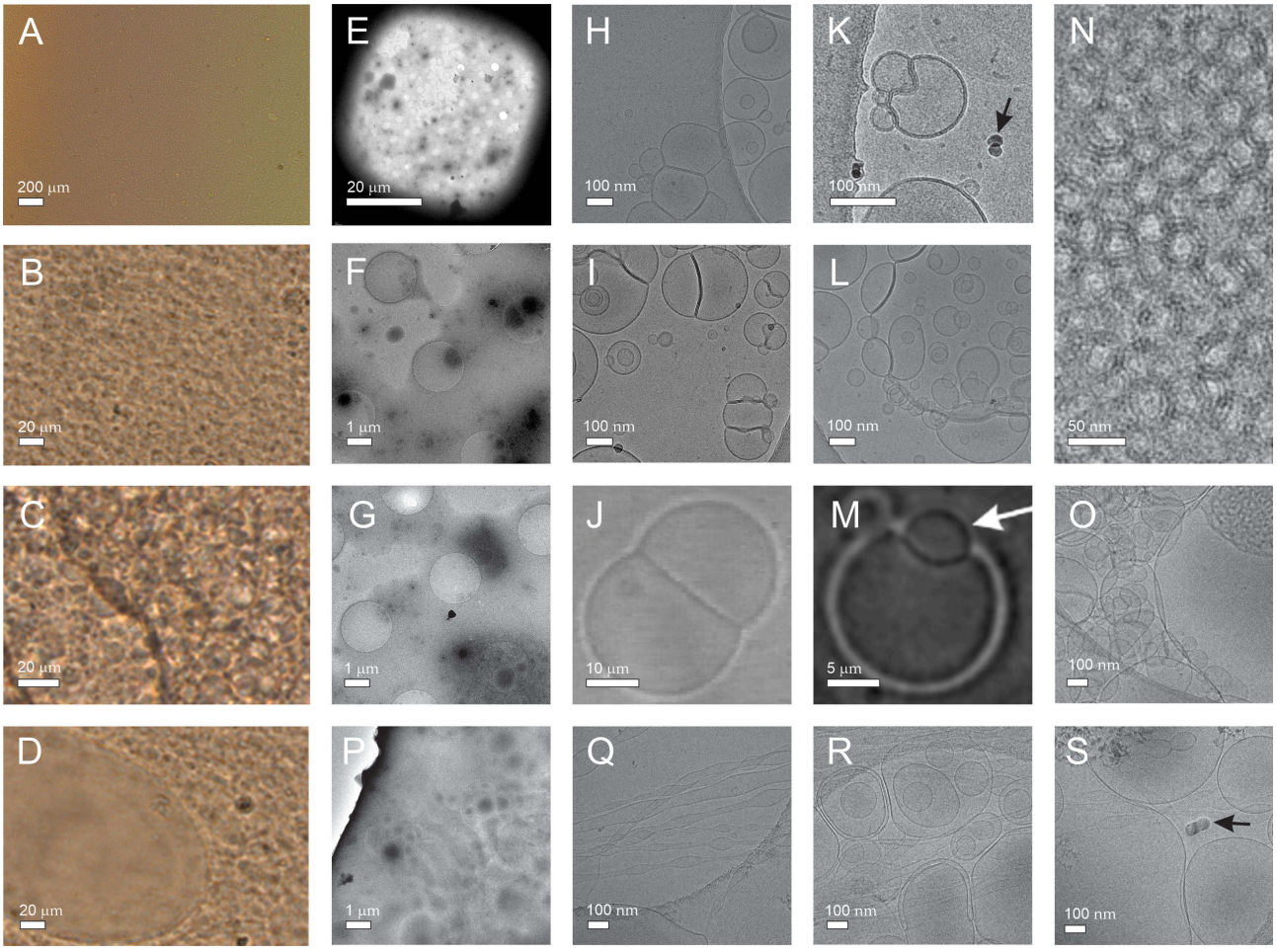

Figure 2 NSHs composed by mixing soya lecithin, glycerol and supernatant from spruce needle homogenate.
Notes: (**A**–**C**) Light microscopy images of undiluted sample, (**D**) sample diluted with water. (**E**–**I**), (**K, L** and **N**–**S**) Cryogenic transmission electron microscopy images of sample diluted 50 000x. Samples P-S were aged 6 months. Black arrows point to electron-dense particles. (**J** and **M**) Light microscopy images of giant unilamellar phospholipid vesicles. (**J**) Reprinted with permission from Tomsiè N, Babnik B, Lombardo D, et al. Shape and size of giant unilamellar phospholipid vesicles containing cardiolipin. *J Chem Inf Model.* 2005;45(6):1676–1679. Copyright 2005 American Chemical Society[56] and reprinted from Volume 150/Edition 1. (**M**) Reprinted with permission from Urbanija J, Tomsic N, Lokar M, et al. Coalescence of phospholipid membranes as a possible origin of anticoagulant effect of serum proteins. *Chem Phys Lipids.* 2007;150:49–57. Copyright 2007 Elsevier.[57] Images of EVs in supernatant from spruce needle homogenate (SW) can be seen in Jeran et al.[46]

engulfed by the larger one, both in NSHs and in giant unilamellar vesicles while keeping both bilayers preserved (Panels L and M, respectively). A stable "non-lamellar" lipid phase composed of a large number of equal-sized small vesicles in close contact was observed (Panels N, O). Panels P-S show samples aged 6 months. Lower magnification image of 6 months aged sample (Panel P) appears similar as the images of fresh samples (Panels E-G). At higher magnification, however, we did not observe adhesion of vesicles to each other (Panels Q-S). Elongated structures (Panels Q-S) were coexisting with globular ones (Panels R, S).

Light microscopy and cryogenic transmission electron microscopy images of liposomes prepared from lecithin, water and glycerol are shown in Figure 3. Two types of lecithin were considered: egg lecithin (A-F) and soya lecithin (G-L). For observation with light microscopy, samples were undiluted (A, G, H) or diluted 3× (B) while for observation with cryogenic transmission electron microscopy, the samples were diluted with water 50,000 ×. Light microscopy images of samples composed of soya lecithin, water and glycerol (Figure 3K and L) are similar to light microscopy images of liposomes composed of soya lecithin, supernatant of spruce needle homogenate, and glycerol (Figure 2A–D). Images of samples composed of egg lecithin, water and glycerol show higher number of larger entities (of the order of 100 μm) (Figure 3A and B).

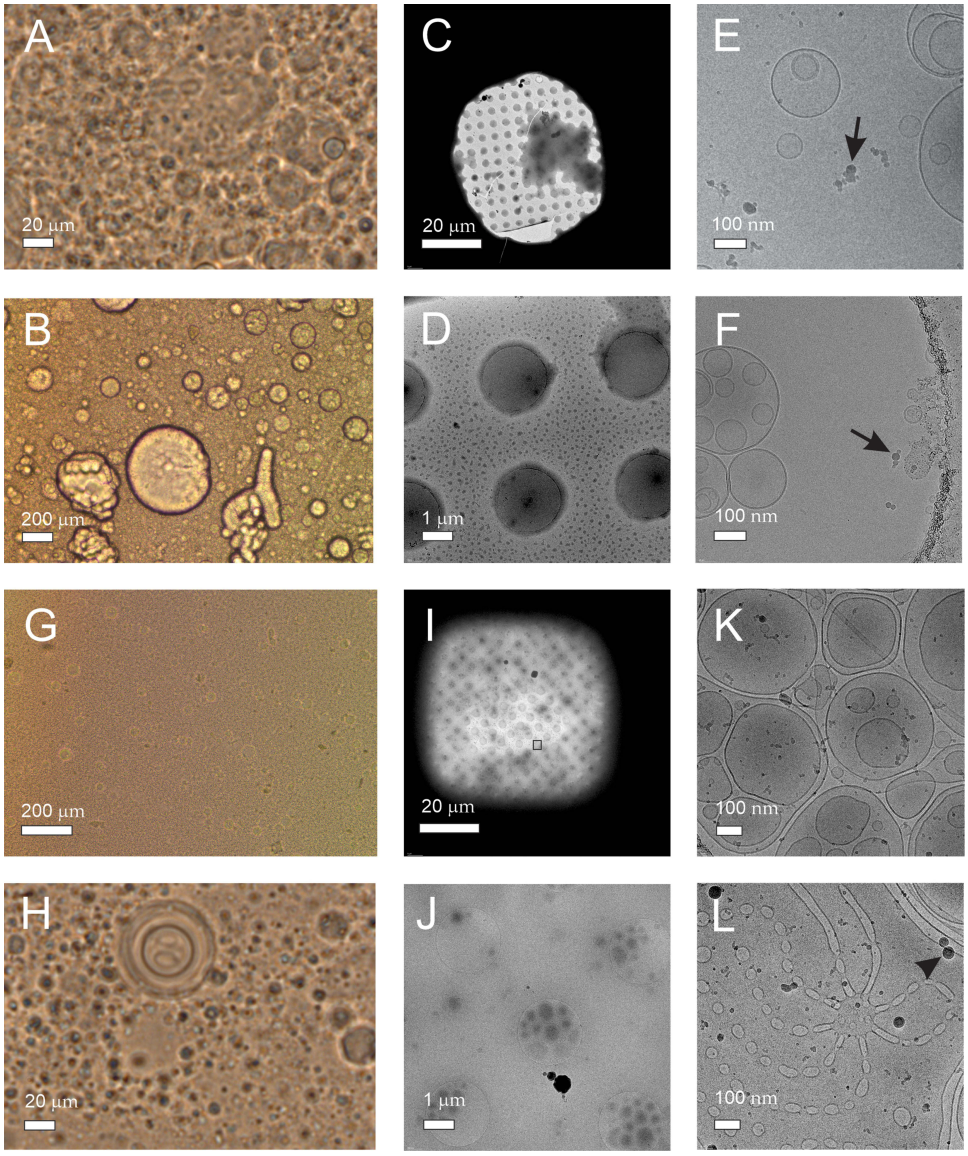

Figure 3 Liposomes composed by mixing lecithin, glycerol and water.
Notes: (**A**) Light microscopy image of undiluted sample composed of egg lecithin, glycerol and water. (**B**) Light microscopy image of sample composed of egg lecithin, glycerol and water, diluted 3×. (**C–F**) Cryogenic transmission electron microscopy images of sample composed of egg lecithin, glycerol and water, diluted 50,000×. (**G** and **H**) Light microscopy images of undiluted sample composed of soya lecithin, glycerol and water, (**I–L**) cryogenic transmission electron microscopy images of sample composed of soya lecithin, glycerol and water. Black arrows and a black triangle point to electron-dense particles.

The average hydrodynamic radius (R_h) of the particles in the NSH and liposome samples was determined by both, dynamic light scattering and interferometric light microscopy techniques. Large (micrometer-sized) particles cause strong scattering of light, therefore the measurement of smaller particles by dynamic light scattering is not possible if the sample contains such particles. Before the measurement by dynamic light scattering, the samples were therefore filtered through 450 nm filters to remove micrometer-sized particles that were visible under light microscopy.

Regardless of the presence of glycerol or the lecithin used, two populations were detected in the filtered samples: smaller particles with average $R_{h,1}$ in the range 14–56 nm and larger particles with average $R_{h,2}$ in the range 163–181 nm (Table 1). The measurement of R_h by interferometric light microscopy agreed with the $R_{h,2}$ values obtained by dynamic light scattering within the standard deviation (Table 1).

By interferometric light microscopy, we determined also R_h of the particles in the supernatant of the spruce needle homogenate that was used to form NSHs. The particles were about two times smaller than NSHs and the liposomes (Table 1).

Estimation of the amount of NSHs and liposomes is given in Table 2. We used four different methods (flow cytometry, interferometric light microscopy, dynamic light scattering and ultraviolet–visual spectroscopy). Flow cytometry and interferometric light microscopy give the concentration of particles in the complementary size ranges: flow cytometry in the meso and cell-sized range (between 400 nm and about 10 μm) and interferometric light microscopy in the nano-sized range between (80 nm and 500 nm). These results show that the samples were rich especially with nano-sized particles (Table 2) as the concentration of meso and cell-sized particles is 3–4 orders of magnitude lower than the concentration of smaller particles (Table 2). The supernatant from spruce needle homogenate contained significantly less particles than the NSH or liposome

Table 1 Hydrodynamic Radii of Particles (R_h) in Liposome Samples Assessed with Two Methods: ILM and DLS, and the Number of Tracked Particles (N) Assessed by ILM

	ILM			DLS		
Sample	**Dilution**	**N tracked**	**R_h ± SD (nm)**	**Dilution**	**R_{h1}(nm)**	**R_{h2}(nm)**
SoyaL/SW/G	100,000	715	137 ± 90	1000	32	163
SoyaL/W/G	10,000	1096	150 ± 80	1000	33	164
EggL/SW/G	10,000	1022	149 ± 100	1000	56	181
EggL/W/G	10,000	1060	141 ± 80	1000	14	168
SW	100	988	85 ± 30			

Abbreviations: ILM, interferometric light microscopy; DLS, dynamic light scattering; SoyaL, soya lecithin; EggL, egg lecithin; SW, supernatant of isolation of small cellular particles from spruce needle homogenate; W, water; G, glycerol.

Table 2 Amount of Material in Samples Containing NSHs, Liposomes and EVs from Spruce Needle Homogenate as Detected by Four Methods: FCM, ILM, DLS and UV-Vis

	FCM		ILM		DLS				UV-Vis	
Sample	**N/mL**	**Dilution***	**N/mL**	**Dilution***	**I_{tot} (kHz/mW)**	**I_1/I_{tot}**	**I_2/I_{tot}**	**Dilution***	**Relative Absorbance at 295 nm**	**Dilution***
SoyaL/SW/G	4.9×10^{8}	10,000	1.1×10^{14}	100,000	132	0.12	0.88	1000	0.17	100
SoyaL/W/G	3.2×10^{8}	10,000	4.6×10^{13}	10,000	47.8	0.12	0.88	1000	0.14	100
EggL/SW/G	1.3×10^{10}	10,000	1.9×10^{13}	10,000	9	0.39	0.61	1000	0.25	100
EggL/W/G	4.2×10^{9}	10,000	3.8×10^{13}	10,000	22.3	0.03	0.97	1000	0.14	100
SW	1.4×10^{7}	100	2.3×10^{11}	100					0.67	1
Protein standard									1	1

Notes: *Dilution factor is depicted as it may affect the number, size and composition of the particles. Reported number densities were corrected for dilution factor. Relative absorbance = Absorbance at 295 nm/Absorbance of Protein standard at the peak of the Absorbance/Wavelength curve (295 nm).

Abbreviations: FCM, flow cytometry; ILM, interferometric light microscopy; DLS, dynamic light scattering; UV-vis, ultraviolet and visual spectroscopy; SoyaL, soya lecithin; SW, supernatant from spruce needle homogenate; W, water; G, glycerol; EggL, Egg lecithin; I, intensity of light scattering.

Table 3 List of the Most Intensive Lipid Species Derived from Spruce Identified in the Hybridosomes

Measured *m/z*	Theoretical *m/z*	Formula	Lipids	Adduct
393.2051	393.2048	$C_{18}H_{35}O_7P$	LPA(15:1), LPA(O-15:2)	$[M-H]^-$
489.2709	489.2708	$C_{23}H_{40}O_8$	2-glyceryl-6-keto-PGF1α	$[M+FA-H]^-$
536.3005	536.2994	$C_{25}H_{48}NO_9P$	LPS(19:1), LPS(O-19:2)	$[M-H]^-$
764.6385	764.6410	$C_{46}H_{89}NO_8$	GalCer(40:1)	$[M-H2O-H]^-$
776.6380	776.6410	$C_{47}H_{89}NO_8$	GlcCer(41:2)	$[M-H2O-H]^-$
808.6644	808.6672	$C_{48}H_{91}NO_8$	GalCer(42:2)	$[M-H]^-$
836.6954	836.6985	$C_{50}H_{95}NO_8$	GalCer(44:2)	$[M-H]^-$
852.6904	852.6934	$C_{50}H_{97}NO_{10}$	GlcCer(44:1)	$[M-H2O-H]^-$
881.6513	881.6512	$C_{53}H_{88}O_7$	DG(50:8)	$[M+FA-H]^-$
894.5904	894.5866	$C_{48}H_{84}NO_9P$	PS(O-42:6)	$[M+FA-H]^-$

samples. In both types of lecithin used, the samples made with supernatant from spruce needle homogenate contained higher amount of proteins than the respective sample prepared with water (Table 1). In dynamic light scattering of samples SoyaL/SW/G, SoyaL/W/G and EggL/SW/G, the population of particles with $R_{h,2}$163–181 nm contributed the most to the total intensity of scattered light (around 90% or more; reported as I_2/I_{tot} in Table 1).

Mass spectrometric measurements revealed rich lipidomic profiles of the spruce homogenate and of the 50,000g supernatant of the EV isolation procedure. In addition, the lipidomic pattern of the supernatant containing the vesicles showed similarities with the lipidomic patterns of the hybridosomes. LC-MS-based lipidomic profiling mainly detected glucosyl- and galactosyl-ceramides derived from spruce in the hybridosomes (Table 3). Besides, lysophosphatidic acids, prostaglandins, lysophosphatidylserines, diacylglycerols and phosphatidylserines were also identified (Table 3).

Mass spectrometry-based proteomic analysis detected the same spruce protein in the spruce homogenate and in the hybridosomes (Accession: A0A117NI30, Description: Uncharacterized protein OS=Picea glauca OX=3330 GN=ABT39_MTgene3847 PE=4 SV=1 PLGS Score: 5127,213, Coverage: 36%).

Discussion

We have composed NSHs from lecithin, glycerol and supernatant from spruce needle homogenate. Visualization of samples with light microscopy and cryogenic transmission electron microscopy showed that the samples contained membrane-enclosed vesicles of different sizes. The smallest hydrodynamic radius (14 nm) was determined by dynamic light scattering in the samples composed from egg lecithin, glycerol and water, while the largest particles were observed by light microscopy (of the order of hundred μm). As no instrument is fit to assess the size and the concentration over such a broad scale range, we used two techniques to measure the hydrodynamic radius of the particles (interferometric light microscopy and dynamic light scattering) and two techniques to measure the concentration of particles: Flow cytometry for meso and cell-sized particles and interferometric light microscopy for nanoparticles. Interferometric light microscopy and dynamic light scattering are not suitable for measuring the concentration of larger particles. It follows from comparison of dynamic light scattering and interferometric light microscopy measurements (Table 2) that the majority of particles were nano-sized. The average R_h values obtained by both, dynamic light scattering (c.f. $R_{h,2}$) and interferometric light microscopy (145–170 nm) were within the experimental error (Table 1). Larger of the two particle populations measured by dynamic light scattering (Table 2) contributed the major part to I_{tot} in three out of four samples. In one of the samples (the sample EggL/SW/G composed of egg lecithin, glycerol and supernatant from spruce needle homogenate), there was a considerable contribution of smaller particles (with radii in the range of a few tens of nanometers) (c.f. $R_{h,1}$ = 56 nm in Table 2). The NSHs as measured with interferometric light microscopy demonstrated higher concentrations than liposomes (Table 2).

Several factors influence the yield of EVs in isolates from cell cultures, such as cell type, cell confluence level, isolation process, assessment procedures and culture conditions.[58] Also, the amount of proteins obtained in isolates of EVs differs significantly across the isolation methods used.[59,60] While the reported yields are expressed in terms of the concentration of EVs, concentration of proteins, concentration of proteins per weight, etc., it is also interesting to know what is the respective volume of the isolate. As described in Jeran et al,[46] isolation of EVs by differential ultracentrifugation starts with 300 mL of sample, the second centrifugation at 300 g retains 240 mL, the first centrifugation at 2000 g retains 180 mL and the second centrifugation at 2000 g retains 120 mL of sample. Isolation continues in the ultracentrifuge which accommodated tubes containing 6 mL of sample (20 tubes). The volume of the isolate (the pellet after ultracentrifugation) in each tube is of the order of 50 µL. This would yield about 1 mL of the isolate, which is less than 1% of the volume of the initial sample.

To estimate the relative proportion of vesicle volume in the isolate to the volume of the raw sample in our NSH and liposome samples, we assume that the vesicles are spherical and consider the average radii of the vesicles as determined by ILM (Table 1). Then if we roughly assume that the vesicles are spherical, the volume of a representative vesicle could be calculated by the formula $V_1 = 4\pi R_h^3/3$. With the number of NSHs in one milliliter depicted in Table 2, the estimated volumes of the vesicles ($V = V_1N$) in proportion to the volume of the sample (1 milliliter) would be 120% (SoyaL/SW/G), 65% (SoyaL/W/G), 26% (EggL/SW/G) and 46% (EggL/W/G). Although this estimation is very rough (there is a distribution of particles over the size, the particles are not spherical, the measurements of size and number are subject to errors), it indicates that the proportion of the volume of NSHs largely exceeds the proportion of the volume of EVs isolated from natural sources (less than 1%).

The choice of methods for harvesting and characterization of EVs is important since processing may considerably affect the samples. Presently acknowledged EV isolation methods include ultrafiltration, size-exclusion chromatography, ultracentrifugation, gradient separation, immuno-affinity capture and commercial reagents.[60] A meta-analysis including 259 studies of cell culture supernatants showed that the majority (90%) of reported isolations were performed by ultracentrifugation. The second most used isolation method (11%) was commercial reagents, while other methods accounted for less than 3% each.[58] In order to enable the use in therapy, a comprehensive physicochemical characterization should be elaborated for every drug nanocarrier and its interactions in biological environments must be thoroughly investigated.

The particles are usually characterized by the size distribution and concentration. Besides a much higher yield, the formation of NSHs has an advantage in fast and simple processing comparing to isolation of EVs from natural sources. Furthermore, samples prepared with supernatant from spruce needle homogenate that were kept at room temperature for 6 months did not significantly differ from fresh samples.[61]

Spruce needle supernatants contained terpenes and flavonoids which are expected to be loaded into NSHs.[46] We have observed the in vivo effect of liposomes and nanohybridosomes on microalgae cultures and found a positive short-term effect on the concentration of microalgae.[62]

Dilution of NSHs with ultraclean water can create differences in the composition of inner and outer solutions. Giant lipid vesicles are sensitive to the osmotic stress caused by different osmolalities of the two solutions which may have caused popping of the vesicles. Respective stability of smaller NSHs is therefore to be investigated in the future.

Efforts are being invested into development of methods for harvesting and characterization of nano-sized particles; however, a golden standard method has not yet been acknowledged. Suspensions of liposomes are dynamic systems subjected to self-assembly according to the minimization of the free energy. They are not particles with fixed identity and are prone to transformations of size, shape and composition during the processing of samples. As flow cytometry involves flow through tubes, it can be expected to have a greater impact on the particle morphology than interferometric light microscopy, dynamic light scattering and ultraviolet–visual spectroscopy methods that are based on scattering of light on the sample. Dynamic light scattering, however, requires filtering which may also have an impact on the particles. Interferometric light microscopy is a recently developed technique based on interference of the incident and the scattered light which was hitherto applied to microorganisms,[63–66] liposomes,[61] extracellular vesicles,[61,66] and isolates from plant homogenate.[46] Besides being minimally invasive, the advantage of this technique is that it gives estimation of the concentration of the particles while dynamic light scattering and ultraviolet–visual spectroscopy give indirect evidence on the abundance of the particles in terms of the intensity of the scattered light and protein/nucleic acid content, respectively. Nanohybridosomes should further be analyzed to define their content, their biological properties, such as cytotoxicity, pH stability, ability to be uptaken by recipient cells and to observe their morphology by high resolution microscopic techniques.

For particles larger than cca 400 nm, flow cytometry proves a convenient method, however, it is also being used for assessment of EVs. For more details please see Welsh et al.[67]

As for the loading into liposome systems, lipophilic cargoes can be inserted within the phospholipid environment, while hydrophilic cargoes can be inserted within the aqueous mediums and then passively incorporated into the liposomes during the hydration process. Further studies are needed to show how the active compounds from *Picea abies* have been incorporated into NSHs, the ability of recipient cells to uptake NSHs, their toxicity, stability and biological activity.

Several liposome-based drug delivery systems have already been approved by the Food and Drug Administration (FDA), and many liposome-based formulations are now in different phases of clinical investigation. However, their physical and chemical stability remains a challenge. NSHs considered in this work maintained size and concentration at room temperature over 6 months' period, which is promising, but studies of their stability with respect to temperature, pH, presence of different compounds in the suspensions and mechanical stress should be performed.

As liposome products are complex and diverse, the procedure of their manufacturing, analysis and control of their physicochemical and biological characteristics should be elaborated to ensure safety and quality of the final products.

Conclusion

We have found that the lipid bilayers (formed by mixing lecithin with aqueous phase containing disintegrated spruce needle cells and glycerol) entrapped the spruce lipids and proteins, thus forming hybrid particles. The majority of these particles were sub-micron sized and were thus called – nanohybridosomes. We present for the first time a systematic study of nanohybridosomes assessing their size, concentration, morphology and lipid/protein content.

Natural samples contain substances that were proved to have beneficial properties; however, efficient delivery of these substances presents a bottleneck to clinically relevant methods. New technologies and principles are being explored to overcome these obstacles. Poor yield of natural sources and biases in small particle assessment methods are the major obstacles to clinical use of EVs which were addressed in this work. We found that the estimated yield of nanohybridosomes (by means of the volume) of the procedure described in our method was more than 25% which is considerably more than the estimated yield of isolation of natural EVs (less than 1%). Follow-up and examination of NSHs' content remain a subject of further investigation.

Funding

This research was funded by Slovenian Research Agency, grant numbers P2-0232, P3-0388, P1-0201, P1-0391, J3-3066, L3-2621, J2-4447, J2-4427 and IO-0003. Project no. SNN 138407 has been implemented with the support provided by the Ministry of Innovation and Technology of Hungary from the National Research, Development and Innovation Fund, financed under the SNN_21 funding scheme. The first and the second authors (Vesna Spasovski and Anna Romolo) contributed equally to the work. The last two authors (Ksenija Kogej and Veronika Kralj-Iglič contributed equally to the work.

Disclosure

The authors report no conflicts of interest in this work.

References

1. Kooijmans SAA, Vader P, van Dommelen SM, van Solinge WW, Schiffelers RM. Exosome mimetics: a novel class of drug delivery systems. *Int j Nanomed*. 2012;7:1525–1541. doi:10.2147/IJN.S29661
2. Abels ER, Breakefield XO. Introduction to extracellular vesicles: biogenesis, RNA cargo selection, content, release, and uptake. *Cell Mol Neurobiol*. 2016;36(3):301–312. doi:10.1007/s10571-016-0366-z
3. Bao G, Mitragotri S, Tong S. Multifunctional nanoparticles for drug delivery and molecular imaging. *Annu Rev Biomed Eng*. 2013;15:253–282. doi:10.1146/annurev-bioeng-071812-152409
4. Fais S, O'Driscoll L, Borras FE, et al. Evidence-based clinical use of nanoscale extracellular vesicles in nanomedicine. *ACS Nano*. 2016;10 (4):3886–3899. doi:10.1021/acsnano.5b08015
5. Mashima R, Takada S. Lipid nanoparticles: a novel gene delivery technique for clinical application. *Curr Issues Mol Biol*. 2022;44(10):5013–5027. doi:10.3390/cimb44100341
6. Yáñez-Mó M, Siljander PR-M, Andreu Z, et al. Biological properties of extracellular vesicles and their physiological functions. *J Extracell Vesicles*. 2015;4:27066. doi:10.3402/jev.v4.27066
7. Burnouf T, Agrahari V, Agrahari V. Extracellular vesicles as nanomedicine: hopes and hurdles in clinical translation. *Int J Nanomed*. 2019;14:8847–8859. doi:10.2147/IJN.S225453

8. Zhang Y, Dou Y, Liu Y, et al. Advances in therapeutic applications of extracellular vesicles. *Int J Nanomed*. 2023;18:3285–3307. doi:10.2147/IJN.S409588
9. Yuan YG, Wang JL, Zhang YX, Li L, Reza AMMT, Biogenesis GS. Composition and potential therapeutic applications of mesenchymal stem cells derived exosomes in various diseases. *Int J Nanomed*. 2023;18:3177–3210. doi:10.2147/IJN.S407029
10. Dong J, Wu B, Tian W. Preparation of apoptotic extracellular vesicles from adipose tissue and their efficacy in promoting high-quality skin wound healing. *Int J Nanomed*. 2023;18:2923–2938. doi:10.2147/IJN.S411819
11. Jing S, Li H, Xu H. Mesenchymal stem cell derived exosomes therapy in diabetic wound repair. *Int J Nanomed*. 2023;18:2707–2720. doi:10.2147/IJN.S411562
12. Kim SJ, Puranik N, Yadav D, Jin JO, Lee PC. Lipid nanocarrier-based drug delivery systems: therapeutic advances in the treatment of lung cancer. *Int J Nanomed*. 2023;18:2659–2676. doi:10.2147/IJN.S406415
13. Emam SE, Ando H, Abu Lila AS, et al. A novel strategy to increase the yield of exosomes (Extracellular Vesicles) for an expansion of basic research. *Biol Pharm Bull*. 2018;41(5):733–742. doi:10.1248/bpb.b17-00919
14. Kurbangaleeva SV, Syromiatnikova VY, Prokopeva AE, et al. Increased yield of extracellular vesicles after cytochalasin B treatment and vortexing. *Curr Issues Mol Biol*. 2023;45:2431–2443. doi:10.3390/cimb45030158
15. Nsairat H, Khater D, Sayed U, Odeh F, Al Bawab A, Alshaer W. Liposomes: structure, composition, types, and clinical applications. *Heliyon*. 2022;8(5):e09394. doi:10.1016/j.heliyon.2022.e09394
16. Betz G, Aeppli A, Menshutina N, Leuenberger H. In vivo comparison of various liposome formulations for cosmetic application. *Int J Pharm*. 2005;296(1–2):44–54. doi:10.1016/j.ijpharm.2005.02.032
17. Budai L, Kaszás N, Gróf P, et al. Liposomes for topical use: a physico-chemical comparison of vesicles prepared from egg or soy lecithin. *Sci Pharm*. 2013;81(4):1151–1166. doi:10.3797/scipharm.1305-11
18. Lombardo D, Kiselev MA. Methods of liposomes preparation: formation and control factors of versatile nanocarriers for biomedical and nanomedicine application. *Pharmaceutics*. 2022;14(3):543. doi:10.3390/pharmaceutics14030543
19. Monteiro N, Martins A, Reis RL, Neves NM. Liposomes in tissue engineering and regenerative medicine. *J R Soc Interface*. 2014;11(101):20140459. doi:10.1098/rsif.2014.0459
20. Takahashi M, Inafuku K, Miyagi T, et al. Efficient preparation of liposomes encapsulating food materials using lecithins by a mechanochemical method. *J Oleo Sci*. 2006;56(1):35–42. doi:10.5650/jos.56.35
21. Zhang N, Ping QN, Huang GH, Xu WF. Investigation of lectin-modified insulin liposomes as carriers for oral administration. *Int J Pharm*. 2005;294(1–2):247–259. doi:10.1016/j.ijpharm.2005.01.018
22. Meure LA, Foster NR, Dehghani F. Conventional and dense gas techniques for the production of liposomes: a review. *AAPS Pharm Sci Tech*. 2008;9(3):798–809. doi:10.1208/s12249-008-9097-x
23. Dhiman N, Awasthi R, Sharma B, Kharkwal H, Kulkarni GT. Lipid nanoparticles as carriers for bioactive delivery. *Front Chem*. 2021;9:580118. doi:10.3389/fchem.2021.580118
24. Huyan T, Hongduo L, Peng H, et al. Extracellular vesicles – advanced nanocarriers in cancer therapy: progress and achievements. *Int j Nanomed*. 2020;15:6485–6502. doi:10.2147/IJN.S238099
25. Le TT, Andreadakis Z, Kumar A, et al. The COVID-19 vaccine development landscape. *Nat Rev Drug Discov*. 2020;19(5):305–306. doi:10.1038/d41573-020-00151-8
26. Estes S, Konstantinov K, Young JD. Manufactured extracellular vesicles as human therapeutics: challenges, advances, and opportunities. *Curr Opin Biotechnol*. 2022;77:102776. doi:10.1016/j.copbio.2022.102776
27. Herrmann IK, Wood MJA, Fuhrmann G. Extracellular vesicles as a next-generation drug delivery platform. *Nat Nanotechnol*. 2021;16(7):748–759. doi:10.1038/s41565-021-00931-2
28. Piffoux M, Silva AKA, Wilhelm C, Gazeau F, Tareste D. Modification of extracellular vesicles by fusion with liposomes for the design of personalized biogenic drug delivery systems. *ACS Nano*. 2018;12(7):6830–6842. doi:10.1021/acsnano.8b02053
29. Belliveau NM, Huft J, Lin PJ, et al. Microfluidic synthesis of highly potent limit-size lipid nanoparticles for in vivo delivery of siRNA. *Mol Ther Nucleic Acids*. 2012;1(8):e37. doi:10.1038/mtna.2012.28
30. Maurer N, Wong KF, Stark H, et al. Spontaneous entrapment of polynucleotides upon electrostatic interaction with ethanol-destabilized cationic liposomes. *Biophys J*. 2001;80(5):2310–2326. doi:10.1016/S0006-3495(01)76202-9
31. Marcus ME, Leonard JN. FedExosomes: engineering therapeutic biological nanoparticles that truly deliver. *Pharmaceuticals Basel*. 2013;6(5):659–680. doi:10.3390/ph6050659
32. Rome S. Biological properties of plant-derived extracellular vesicles. *Food Funct*. 2019;10(2):529–538. doi:10.1039/C8FO02295J
33. Woith E, Guerriero G, Hausman JF, et al. Plant extracellular vesicles and nanovesicles: focus on secondary metabolites, proteins and lipids with perspectives on their potential and sources. *Int J Mol Sci*. 2021;22(7):3719. doi:10.3390/ijms22073719
34. Choi J, Lee DH, Jang H, Park SY, Seol JW. Naringenin exerts anticancer effects by inducing tumor cell death and inhibiting angiogenesis in malignant melanoma. *Int J Med Sci*. 2020;17(18):3049–3057. doi:10.7150/ijms.44804
35. Ju S, Mu J, Dokland T, et al. Grape exosome-like nanoparticles induce intestinal stem cells and protect mice from DSS-induced colitis. *Mol Ther*. 2013;21(7):1345–1357. doi:10.1038/mt.2013.64
36. Liu B, Lu Y, Chen X, et al. Protective role of shiitake mushroom-derived exosome-like nanoparticles in D-galactosamine and lipopolysaccharide-induced acute liver injury in mice. *Nutrients*. 2020;12(2):477. doi:10.3390/nu12020477
37. Yepes-Molina L, Pérez-Jiménez MI, Martínez-Esparza M, et al. Membrane vesicles for nanoencapsulated sulforaphane increased their anti-inflammatory role on an in vitro human macrophage. *Model Int J Mol Sci*. 2022;23(4):1940. doi:10.3390/ijms23041940
38. Kamaitytė-Bukelskienė L, Ložienė K, Labokas J. Dynamics of isomeric and enantiomeric fractions of pinene in essential oil of Picea abies annual needles during growing season. *Molecules*. 2021;26(8):2138. doi:10.3390/molecules26082138
39. Gupta A, Jeyakumar E, Lawrence R. Journey of limonene as an antimicrobial agent. *J Pure Appl Microbiol*. 2021;15(3):1094–1110. doi:10.22207/JPAM.15.3.01
40. van Zyl RL, Seatlholo ST, van Vuuren SF, Viljoen AM. The biological activities of 20 nature identical essential oil constituents. *J Essent Oil Res*. 2006;18(1):129–133. doi:10.1080/10412905.2006.12067134
41. Aydin E, Türkez H, Geyikoğlu F. Antioxidative, anticancer and genotoxic properties of α-pinene on N2a neuroblastoma cells. *Biologia*. 2013;68:1004–1009. doi:10.2478/s11756-013-0230-2

42. Bae GS, Park KC, Choi SB, et al. Protective effects of alpha-pinene in mice with cerulein-induced acute pancreatitis. *Life Sci*. 2012;91(17–18):866–871. doi:10.1016/j.lfs.2012.08.035
43. Kovač J, Šimunović K, Wu Z, et al. Antibiotic resistance modulation and modes of action of (-)-α-pinene in Campylobacter jejuni. *PLoS One*. 2015;10(4):e0122871. doi:10.1371/journal.pone.0122871
44. Salehi B, Upadhyay S, Erdogan Orhan I, et al. Therapeutic potential of α- and β-pinene: a miracle gift of nature. *Biomolecules*. 2019;9(11):738. doi:10.3390/biom9110738
45. Zhang Z, Guo S, Liu X, Gao X. Synergistic antitumor effect of α-pinene and β-pinene with paclitaxel against non-small-cell lung carcinoma (NSCLC). *Drug Res*. 2015;65(4):214–218. doi:10.1055/s-0034-1377025
46. Jeran M, Božič D, Urban N, et al. European spruce (Picea Abies) as a possible sustainable source of cellular vesicles and biologically active compounds. *Proc Socrat Lect*. 2021;5:104–113.
47. Kralj-Iglič V, Arrigler V, Bedina Zavec A, et al. Raw data on interferometric light microscopy assessment of small cellular particles isolated from blood plasma, washed erythrocytes, spruce needle homogenate, suspension of flagellae of microalgae Tetraselmis chuii, conditioned culture media of microalgae Phaeodactylum tricornutum and liposomes; 2020.
48. Kralj-Iglič V, Hočevar M, Iglič A, Jeran M, Romolo A. Scanning electron microscope images of spruce needle homogenate and scanning electron microscope images of isolated small cellular particles from spruce needle homogenate [Data set]. *Int J Mol Sci*. 2023;1. doi:10.5281/zenodo.7437856
49. Mantile F, Kisovec M, Adamo G, et al. A novel localization in human large extracellular vesicles for the EGF-CFC founder member CRIPTO and its biological and therapeutic implications. *Cancers*. 2022;14(15):3700. doi:10.3390/cancers14153700
50. Łukawski M, Dałek P, Borowik T, et al. New oral liposomal vitamin C formulation: properties and bioavailability. *J Liposome Res*. 2020;30(3):227–234. doi:10.1080/08982104.2019.1630642
51. Škufca D, Božič D, Hočevar M, et al. Interaction between Microalgae *P. tricornutum* and Bacteria *Thalassospira Sp*. For Removal of Bisphenols from Conditioned Media. *Int J Mol Sci*. 2022;23(15):8447. doi:10.3390/ijms23158447
52. Schärtl W. *Light Scattering from Polymer Solutions and Nanoparticle Dispersions*. Berlin, Heidelberg: Springer Verlag; 2007.
53. Kratochvil P. Particle scattering functions. In: Huglin MB, editor. *Particle Scattering Functions in Light Scattering from Polymer Solutions*. London and New York: Academic Press Inc; 1972:333–384.
54. Bickel WS, Yousif HA, Bailey WM. Masking of information in light scattering signals from complex scatterers. *Aerosol Sci Technol*. 1982;1:329–335. doi:10.1080/02786828208958598
55. Kato H, Nakamura A, Kinugasa S. Effects of angular dependency of particulate light scattering intensity on determination of samples with bimodal size distributions using dynamic light scattering methods. *Nanomaterials*. 2018;8(9):708. doi:10.3390/nano8090708
56. Tomsiè N, Babnik B, Lombardo D, et al. Shape and size of giant unilamellar phospholipid vesicles containing cardiolipin. *J Chem Inf Model*. 2005;45(6):1676–1679. doi:10.1021/ci050188b
57. Urbanija J, Tomsic N, Lokar M, et al. Coalescence of phospholipid membranes as a possible origin of anticoagulant effect of serum proteins. *Chemist Phys Lipid*. 2007;150(1):49–57. doi:10.1016/j.chemphyslip.2007.06.216
58. Gudbergsson JM, Johnsen KB, Skov MN, Duroux M. Systematic review of factors influencing extracellular vesicle yield from cell cultures. *Cytotechnology*. 2016;68(4):579–592. doi:10.1007/s10616-015-9913-6
59. Brennan K, Martin K, FitzGerald SP, et al. A comparison of methods for the isolation and separation of extracellular vesicles from protein and lipid particles in human serum. *Sci Rep*. 2020;10(1):1039. doi:10.1038/s41598-020-57497-7
60. Momen-Heravi F, Balaj L, Alian S, et al. Current methods for the isolation of extracellular vesicles. *Biol Chem*. 2013;394(10):1253–1262. doi:10.1515/hsz-2013-0141
61. Romolo A, Jan Z, Bedina Zavec A, et al. Assessment of small cellular particles from four different natural sources and liposomes by interferometric light microscopy. *Int J Mol Sci*. 2022;23(24):15801. doi:10.3390/ijms232415801
62. Romolo A, Hočevar M, Iglič A, Griessler Bulc T, Kralj-Iglič V. Short term effect of plant hybridosomes on growth of phaeodactylum tricornutum culture. *Proceed Socrat Lect*. 2023;8:74–86.
63. Boccara M, Fedala Y, Bryan CV, Bailly-Bechet M, Bowler C, Boccara AC. Full-field interferometry for counting and differentiating aquatic biotic nanoparticles: from laboratory to Tara Oceans. *Biomed Opt Express*. 2016;7(9):3736–3746. doi:10.1364/BOE.7.003736
64. Roose-Amsaleg C, Fedala Y, Vénien-Bryan C, Garnier J, Boccara AC, Boccara M. Utilization of interferometric light microscopy for the rapid analysis of virus abundance in a river. *Res Microbiol*. 2017;168(5):413–418. doi:10.1016/j.resmic.2017.02.004
65. Turkki V, Alppila E, Ylä-Herttuala S, Lesch HP. Experimental evaluation of an interferometric light microscopy particle counter for titering and characterization of virus preparations. *Viruses*. 2021;13(5):939. doi:10.3390/v13050939
66. Sausset R, Krupova Z, Guédon E, et al. Comparison of interferometric light microscopy with nanoparticle tracking analysis for the study of extracellular vesicles and bacteriophages. *J Extracell Biol*. 2023;2(2):e75. doi:10.1002/jex2.75
67. Welsh JA, Jones JC, Tang VA. Fluorescence and light scatter calibration allow comparisons of small particle data in standard units across different flow cytometry platforms and detector settings. *Cytometry Part A*. 2020;97A:592–601. doi:10.1002/cyto.a.24029